Organometallic Donor−Acceptor Conjugated Polymer Semiconductors: Tunable Optical, Electrochemical, Charge Transport, and Photovoltaic Properties

Pei-Tzu Wu,[†] Tricia Bull,[‡] Felix S. Kim,[†] Christine K. Luscombe,*[,‡] and Samson A. Jenekhe*[,‡]

Department of Chemical Engineering and Department of Chemistry, University of Washington, Seattle, Washington 98195-1750, and Department of Materials Science and Engineering, University of Washington, Seattle, Washington 98195-2120

Received July 22, 2008; Revised Manuscript Received November 12, 2008

ABSTRACT: A series of 11 organometallic conjugated polymer semiconductors bearing a platinum (Pt) center have been synthesized and their electronic band structures, field-effect charge transport, and use in bulk heterojunction solar cells were evaluated. The Pt-bridged donor−acceptor conjugated poly(aryleneethynylene)s were synthesized by Sonogashira-type polycondensation and are exemplified by poly[4-(5′-*trans*-bis(tributylphosphine)platinum ethynyl-thiophen-2′-yl)-7-(5″-ethynyl-thiophen-2″-yl)-benzo[1,2,5]thiadiazole] (BT-BTPt), poly[5-(5′-*trans*-bis(tributylphosphine)platinum ethynyl-thiophen-2′-yl)-8-(5″-ethynyl-thiophen-2″-yl)-2,3-diheptyl-pyrido[3,4-*b*]pyrazine] (HPP-BTPt), and poly[5-(5′-*trans*-bis(tributylphosphine)platinum ethynyl-thiophen-2′-yl)-7-(5″-ethynyl-thiophen-2″-yl)-thieno[3,4-*b*]pyrazine] (TP-BTPt). The Pt-bridged polymers had reversible electrochemical reduction waves from which electron affinities were found to be 2.95 to 3.28 eV. From the onset oxidation potentials of the polymers, we similarly determined ionization potentials to be 4.82 to 5.23 eV. Optical bandgaps of the donor−acceptor polymers were 1.49 to 1.97 eV. The spin coated polymer thin films showed p-channel field-effect charge transport with average hole mobilities of 3.87 $\times$ 10^{-7} to 3.32 $\times$ 10^{-5} $cm^2/(V\ s)$. Bulk heterojunction solar cells based on blends of the polymers with [6,6]phenyl-C_{71}-butyric acid methyl ester ($PC_{71}BM$) gave power conversion efficiencies as high as 0.68% for HPP-BTPt and 2.41% for BT-BTPt. These results demonstrate the molecular engineering of the electronic band structures and the optical, charge transport, and photovoltaic properties of organometallic donor−acceptor conjugated polymer semiconductors.

Introduction

π-Conjugated polymer semiconductors with donor−acceptor (D–A) architectures are of broad interest for applications in organic electronics and optoelectronics, including light-emitting diodes, field-effect transistors, and photovoltaic cells.[1−8] Through careful design and selection of the donor (D) and the acceptor (A) building blocks, the strength of intramolecular charge transfer (ICT) interaction between the D and A moieties can be selectively tuned to achieve desired optical and electronic properties in conjugated D−A polymer semiconductors.[3,4,5] For example, p-type semiconductors with small bandgaps and broad absorption bands can be designed to facilitate efficient photon harvesting and their electronic properties can be tuned to promote charge separation and transport.[3] Organometallic conjugated polymer semiconductors utilizing the D−A architecture and containing Pt in the backbone have recently been shown to exhibit broad absorption bands and small optical bandgaps suitable for photovoltaics devices.[6,7]

Electron-accepting moieties such as 2,1,3-benzothiadiazole[7] and bithiazole[8] in combination with electron-donating thiophene units have recently been explored in the design of Pt-containing D−A polymer systems. A 2,1,3-benzothiadiazole-containing polymer, BT-BTPt, whose molecular structure is shown in Chart 1, was recently reported to exhibit high power conversion efficiency (PCE) of 4.4−5.0% when blended with [6,6]phenyl-C_{61}-butyric acid methyl ester ($PC_{61}BM$) to make bulk heterojunction solar cells.[7] This efficiency is comparable to the best values for poly(3-hexylthiophene) (P3HT):$PC_{61}BM$ solar cells,

Chart 1

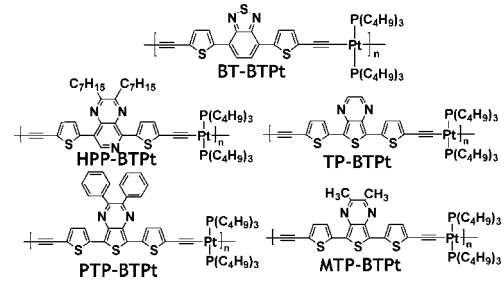

the most efficient and widely studied organic photovoltaic system.[9] However, we note that a controversy has developed regarding the reported efficiencies of BT-BTPt solar cells.[10a] It has been argued on theoretical grounds that the highest power conversion efficiency of BT-BTPt:$PC_{61}BM$ photovoltaic devices with the reported film thickness (70 nm) and experimental optical and electrical data[7] should not be higher than 2.2%.[10a] Nevertheless, a related series of bithiazole-based, Pt-containing poly(aryleneethynylene)s were also recently shown to be promising photovoltaic materials.[8] Bulk heterojunction solar cells based on these later polymers gave an efficiency of up to 2.7% PCE.[8]

In this paper, we report the synthesis, optical and electrochemical properties, field-effect carrier mobilities, and photovoltaic properties of a series of new conjugated organometallic donor−acceptor polymer semiconductors. Eleven organometallic D−A copolymers, whose molecular structures are shown in Chart 1 were synthesized by Sonogashira-type coupling polymerization and investigated, including BT-BTPt (referred to as **P1** in ref 7). Pyrido[3,4-*b*]pyrazine, thieno[3,4-*b*]pyrazines (TP, MTP, PTP), and 2,1,3-benzothiadiazole (BT) were used as the electron acceptors in the series of polymers. The series

* Authors for all correspondence. E-mail: (S.A.J.) jenekhe@u.washington.edu; (C.K.L.) luscombe@u.washington.edu.
[†] Department of Chemical Engineering and Department of Chemistry, University of Washington.
[‡] Department of Materials Science and Engineering, University of Washington.

10.1021/ma8016508 CCC: $40.75
Published on Web 01/13/2009

Chart 2

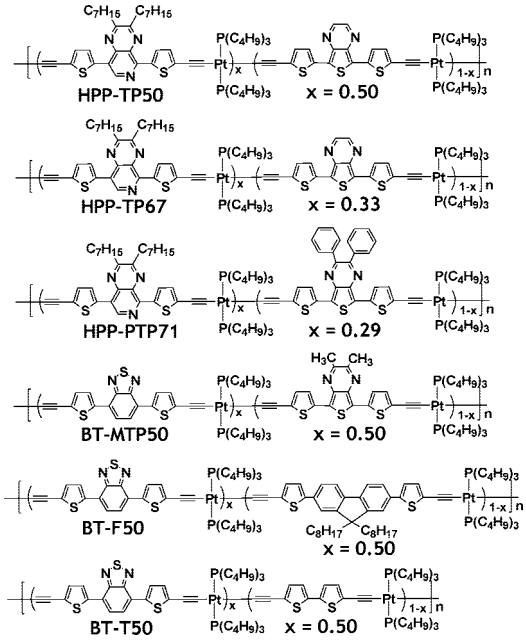

of organometallic D−A polymers include those with one acceptor as shown in Chart 1. Six of the organometallic D−A polymers were random copolymers with two different acceptor building blocks, as shown in Chart 2

The eleven organometallic D−A polymer semiconductors (Charts 1 and 2) share the same architecture of alternating −D−A−D− and −Pt[$P(C_4H_9)_3$]$_2$−, with a fixed 2,5-thienylene donor and varying electron acceptors (A) of pyrido[3,4-*b*]pyrazine (HPP), 2,1,3-benzothiadiazole (BT), and thieno[3,4-*b*]pyrazines (TP, PTP, MTP). We show that these organometallic D−A polymers exhibit strong intramolecular charge transfer and have tunable optical band gaps (1.49−1.97 eV), broad absorption bands that extend to the near-IR region, and ambipolar redox properties with rather small ionization potentials (4.82−5.23 eV). The tunability in photophysical properties and electronic structures of these organometallic D−A copolymers was demonstrated by varying the D−A pairs and the composition in random copolymers. Initial organic field-effect transistors (OFETs) fabricated from the organometallic polymers showed typical p-channel OFET characteristics, and had hole mobilities of up to 3.32×10^{-5} $cm^2/(V\ s)$. Investigation of the photovoltaic properties of the series of polymers showed that BT-BTPt had the highest efficiency of 2.41%.

Experimental Section

Materials. All starting materials and reagents were purchased from Aldrich and used without further purification. 4,7-Dibromobenzo[1,2,5]thiadiazole,[7] 5,8-Dibromo-2,3-diheptyl-pyrido[3,4-*b*]pyrazine,[1a] 5,7-dithiophen-2-yl-thieno[3,4-*b*]pyrazine (**m3**),[11] 2,3-diphenyl-5,7-dithiophen-2-yl-thieno[3,4-*b*]pyrazine (**m4**),[11] 2,3-dimethyl-5,7-dithiophen-2-yl-thieno[3,4-*b*]pyrazine (**m5**),[11] and *trans*-[$PtCl_2(P(C_4H_9)_3)_2$][7] were prepared according to the literature methods.

Synthesis of Polymers. The organometallic D−A polymers shown in Chart 1 were prepared by the polycondensation between *trans*-[$PtCl_2(P(C_4H_9)_3)_2$] and each of **M1**−**M5**. The general procedure for the polymerization was given for BT-BTPt.

Poly[4-(5′-trans-bis(tributylphosphine)platinum ethynyl-thiophen-2′-yl)-7-(5″-ethynyl-thiophen-2″-yl)-benzo[1,2,5]thiadiazole], ***BT-BTPt****.* Polymerization was carried out by mixing **M1** (51.5 mg, 0.15 mmol), *trans*-[$PtCl_2(P(C_4H_9)_3)_2$] (98.9 mg, 0.15 mmol), and CuI (5 mg) in Et_3N/CH_2Cl_2 (42 mL, 1:1, v/v) under N_2. After stirring at room temperature overnight under N_2, the solution was evaporated in vacuo. The purple solid was dissolved in CH_2Cl_2 and filtered through silica gel in order to remove any ionic impurity and residual catalyst. The crude product was further purified by precipitation from CH_2Cl_2 into methanol for several times. After subsequent washing with methanol/hexane and evaporation in vacuo, a dark purple solid of BT-BTPt (104 mg, 74%) was collected. ^{1}H NMR (300 MHz, $CDCl_3$), δ (ppm): 7.99−7.97 (d, 2H), 7.73 (s, 2H), 6.94−6.93 (d, 2H), 2.18−2.13 (m, 12H), 1.64−1.48 (m, 24H), 0.99−0.95 (t, 18H).

Poly[5-(5′-trans-bis(tributylphosphine)platinum ethynyl-thiophen-2′-yl)-8-(5″-ethynyl-thiophen-2″-yl)-2,3-diheptyl-pyrido[3,4-b]pyrazine], ***HPP-BTPt****.* Purple solid. Yield: 613 mg, 92%. ^{1}H NMR ($CDCl_3$), δ (ppm): 8.99 (s, 1H), 8.50 (d, 1H), 7.79 (d, 1H), 6.96 (d, 2H), 3.17−3.07 (m, 4H), 2.18−2.13 (m, 12H), 1.96−2.01 (m, 4H), 1.65−1.36 (m, 40H), 1.0−0.92 (m, 24H).

Poly[5-(5′-trans-bis(tributylphosphine)platinum ethynyl-thiophen-2′-yl)-7-(5″-ethynyl-thiophen-2″-yl)-thieno[3,4-b]pyrazine], ***TP-BTPt****.* Dark green solid. Yield: 506 mg, 81%. ^{1}H NMR ($CDCl_3$), δ (ppm): 8.48−8.42 (d, 2H), 7.45−7.44 (d, 2H), 6.84−6.63 (d, 2H), 2.19−2.16 (m, 12H), 1.64−1.48 (m, 24H), 0.97−0.95 (t, 18H).

Poly[5-(5′-trans-bis(tributylphosphine)platinum ethynyl-thiophen-2′-yl)-7-(5″-ethynyl-thiophen-2″-yl)-2,3-diphenyl-thieno[3,4-b]pyrazine], ***PTP-BTPt****.* Dark green solid. Yield: 180 mg, 41%. ^{1}H NMR ($CDCl_3$), δ (ppm): 7.61−7.57 (m, 4H), 7.52−7.49(m, 2H), 7.39−7.32 (m, 6H), 6.87−6.63 (d, 2H), 2.16−2.04 (m, 12H), 1.71−1.47 (m, 24H), 0.99−0.93 (t, 18H).

Poly[5-(5′-trans-bis(tributylphosphine)platinum ethynyl-thiophen-2′-yl)-7-(5″-ethynyl-thiophen-2″-yl)-2,3-dimethyl-thieno[3,4-b]pyrazine], ***MTP-BTPt****.* Dark blue solid. Yield: 173 mg, 44%. ^{1}H NMR ($CDCl_3$), δ (ppm): 7.44−7.43 (d, 2H), 6.85−6.82 (d, 2H), 2.67−2.64 (s, 6H), 2.17−2.09 (m, 12H), 1.65−1.47 (m, 24H), 1.01−0.87 (t, 18H).

Synthesis of Random Copolymers. The organometallic D−A copolymers shown in Chart 2 were prepared by polycondensation between *trans*-[$PtCl_2(P(C_4H_9)_3)_2$] and the choice of two monomers. The general procedure for the copolymerization is given for HPP-TP50.

Poly[5-(5′-trans-bis(tributylphosphine)platinum ethynyl-thiophen-2′-yl)-8-(5″-ethynyl-thiophen-2″-yl)-2,3-diheptyl-pyrido[3,4-b]pyrazine-co-5-(5′-trans-bis(tributylphosphine)platinum ethynyl-thiophen-2′-yl)-7-(5″-ethynyl-thiophen-2″-yl)-thieno[3,4-b]pyrazine]s, ***HPP-TP50****.* Polymerization was carried out by mixing **M2** (57.6 mg, 0.107 mmol), **M3** (37.2 mg, 0.107 mmol), *trans*-[$PtCl_2(P(C_4H_9)_3)_2$] (143.2 mg, 0.214 mmol), and CuI (5 mg) in Et_3N/CH_2Cl_2 (65 mL, 1:1, v/v) under N_2. After stirring at room temperature overnight under N_2, the solution was evaporated in vacuo. The purple solid was dissolved in CH_2Cl_2 and filtered through silica gel in order to remove any ionic impurity and residual catalyst. The crude product was further purified by precipitation from CH_2Cl_2 into methanol for several times. After subsequent washing with methanol/hexane and evaporated in vacuo, a deep dark purple solid of HPP-TP50 (184 mg, 82%) was collected. ^{1}H NMR (300 MHz, $CDCl_3$), δ (ppm): 8.99 (s, 1H), 8.50 (d, 1H), 8.45 (d, 1.6 H), 7.79 (d, 1H), 7.47 (d, 1.6 H), 6.96 (d, 2H), 6.86 (d, 1.6 H), 3.11 (m, 4H), 2.17 (m, 21.6H), 1.96−2.01 (m, 4H), 1.64−1.34 (m, 59.2 H), 1.0−0.92 (m, 38.4 H). The peaks observed at δ 8.99 and 8.45 ppm can be assigned to the sp^2 CH of the diheptylpyrido[3,4-*b*]pyrazine (HPP) and thieno[3,4-*b*]pyrazine (TP) rings respectively. From the integration of the peaks, the composition ratio (x) can be determined to be 0.56. The real composition is calculated as follows: δ (8.99 ppm, 1H, HPP)/[δ (8.45 ppm, 1.6H, TP) /2 + δ (8.99 ppm, 1H, HPP)].

Poly[5-(5′-trans-bis(tributylphosphine)platinum ethynyl-thiophen-2′-yl)-8-(5″-ethynyl-thiophen-2″-yl)-2,3-diheptyl-pyrido[3,4-b]pyrazine-co-5-(5′-trans-bis(tributylphosphine)platinum ethynyl-thiophen-2′-yl)-7-(5″-ethynyl-thiophen-2″-yl)-thieno[3,4-b]pyrazine]s, ***HPP-TP67****.* The copolymerization was carried out by mixing **M2** (106.5 mg, 0.197 mmol), **M**3 (137.5 mg, 0.394 mmol), *trans*-[$PtCl_2(P(C_4H_9)_3)_2$] (397 mg, 0.592 mmol), and CuI (20.2 mg) in Et_3N/CH_2Cl_2 (150 mL, 1:1, v/v) under N_2. The following workup procedure was the same as reported in the synthesis of HPP-TP50. Yield: 463 mg, 72.9%, dark purple solid. ^{1}H NMR (300 MHz,

$CDCl_3$), δ (ppm): 8.99 (s, 1H), 8.50 (d, 1H), 8.45 (d, 3 H), 7.79 (d, 1H), 7.47 (d, 3 H), 6.96 (d, 2H), 6.86 (d, 3H), 3.11 (m, 4H), 2.17 (m, 30H), 1.96−2.01 (m, 4H), 1.64−1.34 (m, 76 H), 1.0−0.92 (m, 51 H). The peaks observed at δ 8.99 and 8.45 ppm can be assigned to the sp^2 CH of the HPP and TP rings respectively. From the integration of the peaks, the composition ratio (x) can be determined to be 0.40. The real composition is calculated as follows: δ (8.99 ppm, 1H, HPP)/[δ (8.45 ppm, 3H, TP) /2 + δ (8.99 ppm, 1H, HPP)].

Poly[5-(5′-trans-bis(tributylphosphine)platinum ethynyl-thiophen-2′-yl)-8-(5″-ethynyl-thiophen-2″-yl)-2,3-diheptyl-pyrido[3,4-b]pyrazine-co-5-(5′-trans-bis(tributylphosphine)platinum ethynyl-thiophen-2′-yl)-7-(5″-ethynyl-thiophen-2″-yl)-2,3-diphenyl-thieno[3,4-b]pyrazine], ***HPP-PTP71***. The copolymerization was carried out by mixing **M2** (100 mg, 0.185 mmol), **M4** (231.9 mg, 0.463 mmol), *trans*-[$PtCl_2(P(C_4H_9)_3)_2$] (434.8 mg, 0.648 mmol), and CuI (22.1 mg) in Et_3N/CH_2Cl_2 (170 mL, 1:1, v/v) under N_2. The following workup procedure was the similar to that in the synthesis of HPP-TP50. Yield: 380 mg, 53%, dark purple solid. ^{1}H NMR ($CDCl_3$), δ (ppm): 8.99 (s, 1H), 8.50−8.52 (d, 1H), 7.77−7.79 (d, 1H), 7.61−7.57 (m, 3.4 H), 7.52(m, 1.7 H), 7.40 (m, 5.1 H), 6.98 (d, 2H), 6.85 (d, 1.7H), 3.17−3.07 (m, 4H), 2.18−2.01 (m, 26.2 H), 1.62−1.34 (m, 60.4 H), 1.0−0.93 (m, 39.3 H). The peaks observed at δ 8.99 and 6.85 ppm can be assigned to the sp^2 CH of the HPP and PTP rings respectively. From the integration of the peaks, the composition ratio (x) can be determined to be 0.54. The real composition is calculated as follows: δ (8.99 ppm, 1H, HPP)/[δ (6.85 ppm, 1.7H, PTP)/2 + δ (8.99 ppm, 1H, HPP)].

Poly[4-(5′-trans-bis(tributylphosphine)platinum ethynyl-thiophen-2′-yl)-7-(5″-ethynyl-thiophen-2″-yl)-benzo[1,2,5]thiadiazole-co-5-(5′-trans-bis(tributylphosphine)platinum ethynyl-thiophen-2′-yl)-7-(5″-ethynyl-thiophen-2″-yl)-2,3-dimethyl-thieno[3,4-b]pyrazine], ***BT-MTP50***. The copolymerization was carried out by mixing **M1** (75 mg, 0.215 mmol), **M5** (81 mg, 0.215 mmol), *trans*-[$PtCl_2(P(C_4H_9)_3)_2$] (288.7 mg, 0.430 mmol), and CuI (14.7 mg) in Et_3N/CH_2Cl_2 (160 mL, 1:1, v/v) under N_2. The following workup procedure was the similar to the synthesis of HPP-TP50. Yield: 284 mg, 69%, dark purple solid. ^{1}H-NMR ($CDCl_3$), δ (ppm): 8.0 (d, 2H), 7.73 (d, 2H), 7.4 (d, 2H), 6.95 (d, 2H), 6.84 (d, 2H), 2.67−2.64 (s, 6H), 2.18−2.09 (m, 21.6 H), 1.65−1.50 (m, 43.2 H), 1.02−0.97 (t, 32.4 H). The peaks observed at δ 7.73 and 7.4 ppm can be assigned to the sp^2 CH of the thiophene rings closest to the BT and MTP rings respectively. From the integration of the peaks, the composition ratio (x) can be determined to be 0.56. The real composition is calculated as follows: δ (7.73 ppm, 1H)/[δ (7.4 ppm, 3H)/2 + δ (7.73 ppm, 1H)].

Poly[4-(5′-trans-bis(tributylphosphine)platinum ethynyl-thiophen-2′-yl)-7-(5″-ethynyl-thiophen-2″-yl)-benzo[1,2,5]thiadiazole-co-5-(5′-trans-bis(tributylphosphine)platinum ethynyl-thiophen-2′-yl)-7-(5″-ethynyl-thiophen-2″-yl)-9,9-dioctylfluorene-2,7-diyl], ***BT-F50***. The copolymerization was carried out by mixing **M1** (20 mg, 0.057 mmol), **M6** (34.6 mg, 0.057 mmol), *trans*-[$PtCl_2(P(C_4H_9)_3)_2$] (77 mg, 0.114 mmol), and CuI (4 mg) in Et_3N/CH_2Cl_2 (50 mL, 1:1, v/v) under N_2. The following workup procedure was similar to the synthesis of HPP-TP50. Yield: 80 mg, 65%, dark purple solid. ^{1}H NMR (300 MHz, $CDCl_3$), δ (ppm): 7.82 (d, 0.9H), 7.76 (s, 0.9H), 6.65−6.63 (d, 1.1H), 7.55−7.50 (d, 2.2H), 7.25 (d, 1.1H), 6.95 (d, 0.9H), 6.86 (d, 1.1H), 2.18 (m, 12H), 2.02 (m, 2.2H), 1.82−1.52 (m, 24H), 1.07−0.95 (t, 18H and m, 11H), 0.83−0.79 (m, 5.5H). The peak observed at δ 7.82 ppm can be assigned to the two sp^2 CH of the BT unit while the peak at δ 6.65−6.63 ppm can be assigned to the two closest sp^2 CH of the thiophene ring next to the fluorene unit. From the integration of the peaks, the composition ratio (x) can be determined to be 0.45. The real composition is calculated as follows: δ (7.82 ppm, 0.9H)/[δ (7.82 ppm, 0.9H) + δ (6.65−6.63 ppm, 1.1H)].

Poly[4-(5′-trans-bis(tributylphosphine)platinum ethynyl-thiophen-2′-yl)-7-(5″-ethynyl-thiophen-2″-yl)-benzo[1,2,5]thiadiazole-co-5′-trans-bis(tributylphosphine)platinum ethynyl-5-ethynyl-[2,2′]bithiophenyl], ***BT-T50***. The copolymerization was carried out by mixing **M1** (69.4 mg, 0.199 mmol), 5,5′-diethynyl-[2,2′]bithiophenyl (42.7 mg, 0.199 mmol), *trans*-[$PtCl_2(P(C_4H_9)_3)_2$] (267 mg, 0.398mmol), and CuI (13.6 mg) in Et_3N/CH_2Cl_2 (90 mL, 1:1, v/v) under N_2. The following workup procedure was similar to the synthesis of HPP-TP50. Yield: 180 mg, 51%, red purple solid. ^{1}H NMR (300 MHz, $CDCl_3$), δ (ppm): 7.99−7.97 (d, 0.9H), 7.73 (d, 0.9H), 6.94 (d, 0.9H), 6.87 (d, 1.1H), 6.71 (d, 1.1H), 2.21−2.13 (m, 12H), 1.64−1.45 (m, 24H), 0.99−0.93 (t, 18H). The peak observed at δ 7.99−7.97 ppm can be assigned to the sp^2 CH of the BT unit and the peak at δ 6.87 and 6.71 ppm can be assigned to the sp^2 CH of the bithiophene moieties. From the integration of the peaks, the composition ratio (x) can be determined to be 0.45. The real composition is calculated as follows: δ (7.99−7.97 ppm, 0.9H)/[δ (7.99−9.97 ppm, 0.9H) + δ (6.87 ppm, 1.1H)].

Characterization. ^{1}H NMR spectra were recorded on a Bruker-AF300 spectrometer at 300 MHz. UV−vis absorption spectra were recorded on a Perkin-Elmer model Lambda 900 UV/vis/near-IR spectrophotometer. Spin-coated polymer thin films were prepared from 2 wt % solutions in chloroform. The photoluminescence (PL) emission spectra were obtained with a Photon Technology International (PTI) Inc. model QM-2001−4 spectrofluorimeter. Cyclic voltammetry experiments were carried out on an EG&G Princeton Applied Research potentiostat/galvanostat (model 273A) in an electrolyte solution of 0.1 M tetrabutylammonium hexafluorophosphate (Bu_4NPF_6) in acetonitrile. A three-electrode cell was used in all experiments. Platinum wire electrodes were used as both counter and working electrodes, and silver/silver ion (Ag in 0.1 M $AgNO_3$ solution, Bioanalytical System, Inc.) was used as a reference at the beginning of the experiments by running cyclic voltammetry on ferrocene as the internal standard. The potential values obtained in reference to the Ag/Ag^+ electrode were then converted to the saturated calomel electrode (SCE) scale. The films of the polymers were coated onto the platinum working electrode by dipping the platinum wire into a 2 wt % chloroform solution of each polymer sample and dried under vacuum at 60 °C for 1 h.

Fabrication and Characterization of Thin Film Transistors. Heavily n-doped Si substrates with thermally grown 100 or 300 nm SiO_2 were used as gate electrodes and gate dielectric. Source and drain electrodes were patterned by photolithography with Au/Ti layer for bottom-contact devices. The devices have various dimensions with W/L ratios of 10−500, where W is the channel width and L is the channel length. Thin films of the copolymers were prepared by spin-coating a 0.1 wt % or 0.3 wt % chloroform or 1,2-dichlorobenzene solution onto octyltriethoxysilane (OTS-8) vapor treated SiO_2 surface and dried for 10−12 h at room temperature in a vacuum chamber. The polymer film thickness in OFETs was 30−100 nm depending on the polymer and processing conditions and was measured by an Alpha-step 500 profilometer. For top-contact devices, Au source and drain electrodes were evaporated on top of polymer thin-film after spin-coating. Electrical characteristics of the devices were measured on a Keithley 4200 semiconductor parameter analyzer (Keithley Instruments, Inc., Cleveland OH). All the measurements were done under ambient conditions.

Fabrication and Characterization of Photovoltaic Cells. Solar cells were fabricated on ITO coated glass substrates (Colorado Concept Coatings) cleaned using stepwise sonication in detergent, DI water, acetone, and IPA followed by 10 min of O_2 plasma etching. The substrates were coated with poly(3,4-ethylenedioxythiophene):poly(styrene sulfonate), PEDOT:PSS, (Baytron P VP Al 4083), which was spun coat at 4000 rpm for 30 s and annealed at 120 °C for 1 h to yield 40 nm thick films. $PC_{61}BM$ and $PC_{71}BM$ were purchased from American Dye Source and all polymers were synthesized as described herein. Polymer:PCBM solutions were prepared with anhydrous dichlorobenzene (35 mg/mL), heated to 70 °C and stirred overnight in a nitrogen glovebox to dissolve the constituents, and filtered through 0.20 μm PTFE filters. The polymer solutions were spun in a N_2 glovebox at 1000 rpm for 60s resulting in 60−80 nm films. In general, the film thickness of the polymer:PCBM blends in the photovoltaic devices was in the range of 50−80 nm. Active areas of 3.14×10^{-2} cm^2 were defined with by evaporating 1.0 nm of LiF and 80 nm of Al through a shadow

Scheme 1. Synthesis of Organometallic D−A Polymers

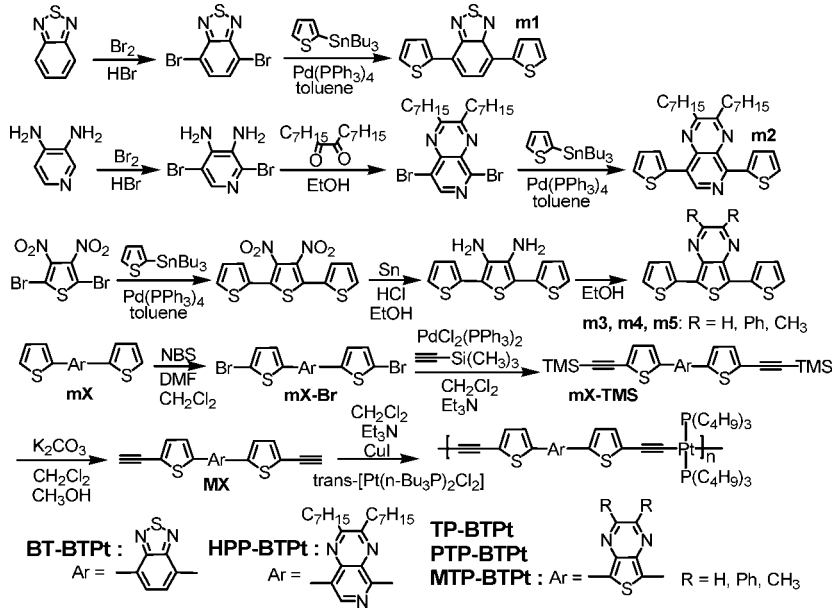

Scheme 2. Synthesis of Organometallic D−A Copolymers

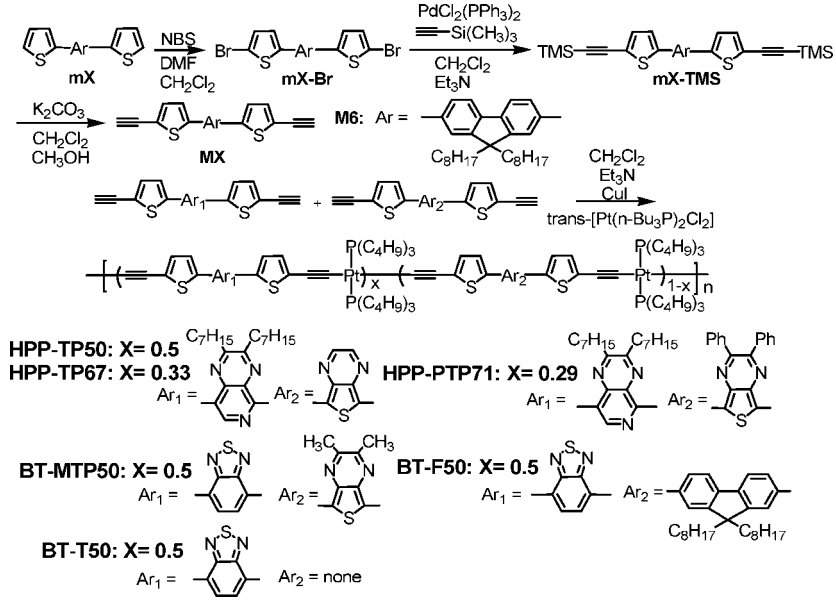

mask at 2×10^{-6} Torr. Devices used for external quantum efficiency measurements were prepared on etched ITO substrates with an active area of 0.2 cm^2. Power conversion efficiency measurements were performed in air using a 450 W Xe Lamp and AM1.5 Filter at 100 W/cm^2 calibrated to an NREL certified silicon reference diode with a KG5 filter and collected with a Keithley 4200.

Results and Discussion

Synthesis and Characterization. The synthetic routes used to prepare the monomers, polymers and copolymers are outlined in Schemes 1 and 2. The monomers **m1** and **m2** were prepared by Stille coupling of 2-tributylstannylthiophene and 4,7-dibromo-benzo[1,2,5]thiadiazole and 5,8-dibromo-2,3-diheptylpyrido[3,4-*b*]pyrazine, respectively. The diamine precursors for **m3**−**m5** were prepared according to the literature method[11] followed by condensation with their corresponding diones to give **m3**−**m5**. Each monomer **m*x*** was reacted with *N*-bromosuccinimide (NBS) in a mixture of CH_2Cl_2 and DMF to afford the dibromide **m*x*-Br** in high yields of 85−90% after recrystallization. Conversion of the dibromide **m*x*-Br** to the corresponding diethylnyl monomer **M*X*** followed the typical alkylnylation procedure for the aromatic halides by first forming **m*x*-TMS**, which was subsequently deprotected.[12] The five organometallic polymers in Chart 1 were synthesized by Sonogashira-type dehalogenation reaction[6] between **M1**−**M5** and *trans*-$[PtCl_2(P(C_4H_9)_3)_2]$. Similarly, the synthesis of six Pt-containing copolymers, such as HPP-TP50, is outlined in Scheme 2. They were prepared by adjusting the feed molar ratio (x) between two monomers (**M1**, **M2**) while maintaining a 1:1 molar ratio between the **M*X*** and *trans*-$[PtCl_2(P(C_4H_9)_3)_2]$. All of the eleven polymers (Charts 1 and 2) were soluble in organic solvents such as chloroform, toluene, and tetrahydrofuran (THF). The chemical structures and actual composition of the copolymers were verified by ^1H NMR in $CDCl_3$. The onset decomposition temperatures (T_d) of the eleven polymers, derived from thermogravimetric analysis (TGA) scans under nitrogen at a heating

Table 1. Molecular Weight and Thermal Properties of Polymers

copolymer	yield (%)	M_w[a]	M_n[a]	M_w/M_n[a]	T_d[b] (°C)
BT-BTPt	74	23700	11300	2.10	337
HPP-BTPt	92	58200	23300	2.50	331
TP-BTPt	81	7800	4000	1.95	280
PTP-BTPt	41	9000	5000	1.80	310
MTP-BTPt	44	11100	5800	1.91	337
HPP-TP50	83	20900	10100	2.07	287
HPP-TP67	73	15400	6600	2.33	298
HPP-PTP71	53	5800	800	7.25	319
BT-MTP50	69	11700	2000	5.85	321
BT-F50	51	18900	10100	1.87	310
BT-T50	65	45700	24300	1.88	302

[a] Molecular weights were determined by GPC using polystyrene standards. [b] Onset decomposition temperature measured from TGA under nitrogen.

rate of 10 °C/min, are in the range of 280 to 337 °C as listed in Table 1, indicative of good thermal stability for this class of polymers. TP-BTPt showed a much lower T_d of 280 °C compared to PTP-BTPt (310 °C) and MTP-BTPt (337 °C) partially because it has a smaller molecular weight.

The molecular weights of the polymers, determined by gel permeation chromatography (GPC) against polystyrene standards in THF, are shown in Table 1. Our BT-BTPt sample has a number-average molecular weight (M_n) of 11300, a weight-average molecular weight (M_w) of 23700, and a molecular weight distribution (M_w/M_n) of 2.10, which are comparable to the reported values (M_n = 11360 g/mol and M_w/M_n = 1.84) in the literature.[7] HPP-BTPt has a M_n of 23300 g/mol with a M_w/M_n of 2.50, and contains an estimated 61 aromatic rings in the conjugated backbone. The thienopyrazine-based copolymers of TP-BTPt, PTP-BTPt, and MTP-BTPt have low M_n of 4000−5800 g/mol. HPP-TP50 and HPP-TP67 from copolymerizing **M2** and **M3** with *trans*-[$PtCl_2(P(C_4H_9)_3)_2$] also have decent M_n of 10100 and 6600 g/mol, respectively. BT-F50 and BT-T50 have quite high M_n of 10100 and 24300 g/mol and their polydispersities are lower than 2.0. HPP-PTP71 and BT-MTP50 exhibit quite low M_n and very broad molecular distributions for unclear reasons. Generally, organometallic copolymers prepared by Sonogashira polycondensation exhibit high molecular weights (M_n > 5000 g/mol) and their moderate molecular weight distributions (M_w/M_n) are close to 2.

Optical Properties. The normalized optical absorption spectra of the organometallic D−A copolymers in dilute (10^{-5} M) dichloromethane solutions are shown in Figure 1A. The absorption spectra of BT-BTPt, HPP-BTPt, TP-BTPt, PTP-BTPt, and MTP-BTPt polymers in dilute solutions (Figure 1A) are characterized by two bands, one at 376−414 nm and the other at 532−655 nm. The former band at the low wavelength region can be assigned to $\pi-\pi^*$ transition whereas the lowest energy band (532−655 nm) is due to ICT interaction between the thiophene donor and the different acceptor moieties. By changing the electron acceptor from 2,3-diheptylpyrido[3,4-*b*]pyrazine (HPP in HPP-BTPt) and 2,1,3-benzothiadiazole (BT in BT-BTPt), to thieno[3,4-*b*]pyrazines (MTP in MTP-BTPt, TP in TP-BTPt, and PTP in PTP-BTPt), a gradual red-shift of the ICT absorption band results with λ_{max} ranging from 532 to 655 nm. The red-shifted absorption bands indicate that the ICT strength increases with acceptor strength.

The absorption spectra of copolymer thin films in Figure 1B are generally similar in shape with those in dilute solutions with distinct $\pi-\pi^*$ transition absorption and ICT absorption bands. A similar red-shift of the lower-energy ICT absorption band with λ_{max} in the range of 543−680 nm from HPP-BTPt to PTP-BTPt, is also observed in the thin film absorption spectra as shown in Figure 1B. The trend in absorption spectra supports the idea of tuning the absorption band over a broad wavelength range by varying the ICT strength of D−A pairs with different electron acceptors from HPP, BT, and MTP to TP and PTP. As a result, the optical-absorption-edge bandgaps of the thieno[3,4-*b*]pyrazines-based polymers TP-BTPt (1.54 eV), PTP-BTPt (1.49 eV), and MTP-BTPt (1.66 eV) are much smaller than those of BT-BTPt (1.86 eV) and HPP-BTPt (1.97 eV), which is characteristic of strong intramolecular charge transfer in the series of D−A polymers.

In the design of copolymers HPP-TP50 and HPP-TP67, two different D−A−D repeating units (Th-HPP-Th and Th-TP-Th) were combined in the random copolymers and connected by the electron-rich Pt-center and alkynyl unit. In Figure 2A, both HPP-TP50 and HPP-TP67 show the $\pi-\pi^*$ absorption bands (378 and 409 nm) and two clear ICT absorption bands at 532−541 nm and 632−643 nm that are reminiscent of HPP-BTPt (D−A−D = Th-PP-Th, 573 nm) and TP-BTPt (D−A−D = Th-TP-Th, 651 nm), respectively. HPP-TP50 has a higher absorption intensity at lower wavelengths (532 nm) than that of HPP-TP67 as a result of increasing composition ratio of **M2** compared to **M3** in the monomer feed. Their thin film absorption spectra are similar in shape but slightly red-shifted as shown in Figure 2B. The theoretical absorption spectrum of HPP-TP67 (labeled as HPP-TP67*) was estimated by addition of the absorption spectra of the constituent polymers HPP-BTPt and TP-BTPt at the composition ratio (0.4:0.6), as shown in Figure 2C. The experimental thin film absorption spectrum of HPP-TP67 is in excellent agreement with that calculated from the components (HPP-TP67*). This demonstrates that we can predict the absorption spectrum of a new copolymer at a given composition ratio of its constituent repeating units. Additionally, HPP-TP50 and HPP-TP67 exhibit small optical bandgaps of 1.55 and 1.54 eV similar to that of TP-BTPt (1.54 eV) because of the presence of the Th-TP-Th (D−A−D) pair. HPP-PTP71 also has a $\pi-\pi^*$ transition band at 372 nm and two ICT absorption bands at 527 and 633 nm that are characteristic of HPP-BTPt (D−A−D = Th-HPP-Th, 532 nm) and PTP-BTPt (D−A−D = Th-PTP-Th, 655 nm) in the solution state (Figure 2A), and HPP-PTP71's optical bandgap of 1.53 eV is similar to that of PTP-BTPt (1.49 eV).

The two absorption bands of BT-MTP50 at 385 and 569 nm (Figure 2A) are a result of both Th-BT-Th and Th-MTP-TP moieties and the lower-energy band is reminiscent of the ICT absorption bands of BT-BTPt (561 nm) and MTP-BTPt (609 nm) shown in Figure 1A. Its thin film absorption bands are red-shifted to 394 and 592 nm (Figure 2B), with an optical bandgap of 1.68 eV. In the case of BT-F50 and BT-T50, their ICT absorption bands at 540 and 546 nm (Figure 2A) are characteristic of Th-BT-Th moieties which is very close to the ICT band (561 nm) in BT-BTPt whereas BT-F50 and BT-T50 have more intense and slightly red-shifted absorption in the lower wavelength region (402 and 398 nm) compared to BT-BTPt (379 nm) due to the thiophene-fluorene and bithiophene repeating units in BT-F50 and BT-T50, respectively. Similarly, their absorption bands are red-shifted to 395/566 nm and 400/577 nm in BT-F50 and BT-T50 as thin films in Figure 2B. Thus, BT-F50 and BT-T50 have almost identical optical bandgaps of 1.89 and 1.88 eV originating from their ICT character of the same Th-BT-Th moieties in the copolymer backbones.

The incorporation of different electron acceptors in BT-BTPt, HPP-BTPt, TP-BTPt, PTP-BTPt, and MTP-BTPt demonstrates the tunability of ICT absorption bands with λ_{max} at a broad wavelength range of 543−680 nm in thin films, as well as a tunable optical bandgap of 1.49−1.97 eV in the solid state (Table 2). Furthermore, the absorption bands are tailored to cover the visible wavelength region in the five copolymers by combining two D−A−D pairs. Also, the relative absorption intensity of two different ICT absorption bands is tuned by

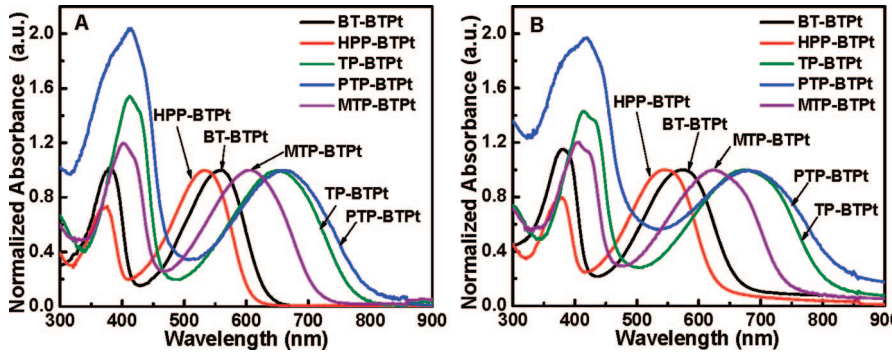

Figure 1. Optical absorption spectra of 10^{-5} M solutions of organometallic polymers in dichloromethane (A) and as thin films (B).

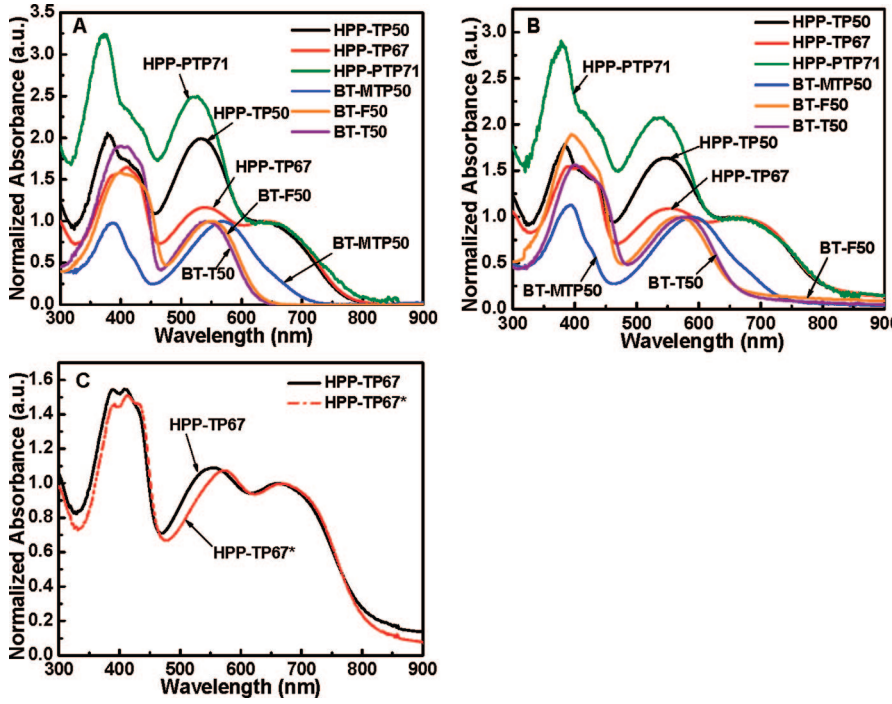

Figure 2. Optical absorption spectra of 10^{-5} M solutions of organometallic copolymers in dichloromethane (A) and as thin films (B). The comparison of the thin film absorption spectrum of HPP-TP67 and the theoretically calculated spectrum for HPP-TP67* (C).

Table 2. Optical, Redox, and Charge Transport Properties of Copolymers

	solution		film									
copolymer	λ_{max}^{abs} (nm)	λ_{max}^{em} (nm)	λ_{max}^{abs} (nm)	λ_{max}^{em} (nm)	E_g^{opt} (eV)	$E_{ox}^{onset a}$ (V)	IP[b] (eV)	$E_{red}^{onset a}$(V)	EA[c](eV)	E_g^{el} (eV)	μ_h (cm^2/(V s))	V_T (V)
BT-BTPt	379, 561	681	380, 572	700	1.86	0.75	5.15	−1.38	3.02	2.13	1.83×10^{-5}	−10.8
HPP-BTPt	376, 532	644	380, 543	648	1.97	0.79	5.19	−1.45	2.95	2.25	6.27×10^{-6}	−14.1
TP-BTPt	412, 651		415, 674		1.54	0.42	4.82	−1.29	3.11	1.71	1.16×10^{-6}	−15.1
PTP-BTPt	414, 655		418, 680		1.49	0.58	4.98	−1.19	3.21	1.77		
MTP-BTPt	402, 609	740	407, 622		1.66	0.56	4.96	−1.37	3.03	1.93	3.32×10^{-5}	−10.3
HPP-TP50	378, 532, 632	635	384, 548, 655		1.55	0.56	4.96	−1.29	3.11	1.85	1.93×10^{-6}	−8.6
HPP-TP67	409, 541, 643	629	408, 552, 661		1.54	0.54	4.94	−1.26	3.14	1.80	7.17×10^{-7}	−7.7
HPP-PTP71	372, 527, 633	637	378, 543, 656		1.53	0.72	5.12	−1.12	3.28	1.84		
BT-MTP50	385, 569	713	394, 592		1.68	0.79	5.19	−1.33	3.07	2.12	1.80×10^{-6}	−12.8
BT-F50	402, 540	676	395, 566	691	1.89	0.83	5.23	−1.31	3.09	2.14	3.87×10^{-7}	−17.1
BT-T50	398, 546	684	400, 577	695	1.88	0.80	5.20	−1.23	3.17	2.03	1.11×10^{-6}	−29.8

[a] Onset oxidation and reduction potentials vs SCE. [b] Ionization potential was obtained based on IP = E_{ox}^{onset} + 4.4 eV [c] Electron affinity was obtained based on EA = E_{red}^{onset} + 4.4 eV.

changing the composition ratio of two D−A−D repeating units. The small optical band gaps and broad absorption bands of these organometallic D−A copolymers suggest that they could be useful materials for photovoltaic applications.[3,7,8]

The normalized photoluminescence (PL) emission spectra of the copolymers in dichloromethane are shown in Figure 3A. The PL spectra of TP-BTPt and PTP-BTPt were too weak and beyond the wavelength range of our instrument detection. BT-BTPt, HPP-BTPt, and MTP-BTPt show broad and featureless PL emission peaks at 681, 644, and 740 nm that originate from their ICT excited states. HPP-BTPt, HPP-TP50, HPP-TP67, and HPP-PTP71 have similar PL emission peaks at 629−644 nm, which originate from their ICT excited states of the same Th-HPP-Th moieties. However, the Th-TP-Th and Th-PTP-Th moieties in HPP-TP50, HPP-TP67, and HPP-PTP71 have no detectable emission in the visible wavelength region. Likewise, BT-BTPt, BT-F50, and BT-T50 have close PL emission peaks at 676−684 nm because they share the same Th-BT-Th moiety

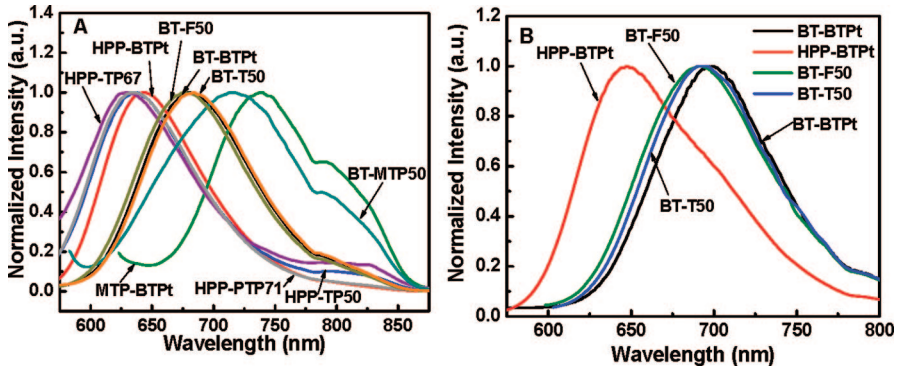

Figure 3. Photoluminescence spectra of organometallic polymers in dichloromethane (A) and as thin films (B).

from which ICT emission originates. BT-MTP50 shows a very broad emission peak at 713 nm that can be assigned to two ICT emissions coming from both Th-BT-Th and Th-MTP-Th moieties. We do not currently know the true origin of a shoulder peak (~790 nm) in the PL emission spectra of BT-MTP50 and MTP-BTPt (Figure 3A); the copolymers HPP-TP50 and HPP-TP67 similarly exhibit weak shoulder bands in the same wavelength region. We speculate that the shoulder peak may be related to energy transfer among the thiophene-dimethylthienopyrazine-thiophene moieties in both BT-MTP50 and MTP-BTPt similar to what was observed in related thienopyrazine-based donor−acceptor copolymers.[5a]

The PL spectra of HPP-BTPt, BT-BTPt, BT-F50, and BT-T50 copolymers thin films are shown in Figure 3B. The other copolymers have no detectable emission in thin films. HPP-BTPt has an emission peak at 648 nm whereas BT-BTPt, BT-F50, and BT-T50 thin films show almost identical ICT emission at 691−700 nm originating from the same Th-BT-Th chromophore.

Electrochemical Properties. The electronic states, ionization potential/electron affinity, HOMO (highest occupied molecular orbital)/LUMO (lowest unoccupied molecular orbital) levels, of the organometallic D−A conjugated polymers were investigated by cyclic voltammetry (CV).[13] The oxidation and reduction cyclic voltammograms of the polymer thin films are shown in Figure 4, and all the electrochemical data are summarized in Table 2. Our BT-BTPt sample has irreversible oxidation and reversible reduction as evident from the areas and close proximity of the anodic and cathodic peaks shown in Figure 4, parts A and B. The onset oxidation potential and onset reduction potential of BT-BTPt are 0.75 and −1.38 eV (vs SCE), respectively, from which we estimate an ionization potential (IP, HOMO level) of 5.15 eV (IP = E_{ox}^{onset} + 4.4),[13] an electron affinity (EA, LUMO level) of 3.02 eV (EA = E_{red}^{onset} + 4.4),[13] and an electrochemical bandgap of 2.13 eV (E_g^{el} = IP − EA). The experimental values of IP, EA, and E_g^{el} of BT-BTPt (measured in the CH_2Cl_2 solution) have been reported to be 5.37, 3.14, and 2.23 eV,[7] which are very similar to our experimental results for thin films.

All of the organometallic D−A copolymers exhibit reversible reduction as shown in parts B−D of Figure 4. The onset reduction potentials (E_{red}^{onset}) and corresponding electron affinities (EAs) for the polymers are listed in Table 2. Compared to the known electron-withdrawing BT moieties in BT-BTPt, the electron-accepting HPP, MTP, TP, and PTP units in the polymer backbones of HPP-BTPt, MTP-BTPt, TP-BTPt, and PTP-BTPt play an important role in their reduction potentials. For example, the thienopyrazines (PTP, TP, and MTP) with stronger electron-accepting ability resulted in higher EA values of 3.03−3.21 eV than an EA of 2.95 eV observed for HPP-BTPt with the weaker HPP electron−accepting moiety. In the case of the random copolymers HPP-TP50 and HPP-TP67 that carry two electron−accepting moieties (HPP and TP), the stronger TP acceptor was found to determine the reduction potentials and led to EAs of 3.11−3.14 eV, which are almost identical to the EA (3.11 eV) of TP-BTPt. The reduction curves of HPP-TP50 and HPP-TP67 exhibit a broad shoulder at −1.65 V and major peaks at −1.95 and −2.15 V (vs SCE) in Figure 4C, which come from the reduction occurring in the TP and HPP moieties. Similarly, HPP-PTP71 exhibits an EA of 3.28 eV, which is very close to that of PTP-BTPt (3.21 eV) because they both bear the strong acceptor PTP in the conjugated backbone. BT-MTP50 contains two comparable electron acceptors (BT and MTP), thus exhibits an EA of 3.07 eV, which is similar to the EAs (3.02 and 3.03 eV) of BT-BTPt and MTP-BTPt. Since BT-F50 and BT-T50 both bear the same BT unit, it is not surprising for them to exhibit EAs of 3.09−3.17 eV, close to that of BT-BTPt. The current intensity of the reduction curves of BT-F50 and BT-T50 are substantially lower that the other polymers because of the small amount of the electron-accepting units in these two copolymers (Figure 4D).

Similar to the irreversible oxidation observed in BT-BTPt, HPP-BTPt also showed an irreversible oxidation CV (Figure 4A) and had an IP of 5.19 eV, which is very close to 5.15 eV seen in BT-BTPt. The stronger electron-accepting thienopyrazine-based polymers, MTP-BTPt, TP-BTPt, and PTP-BTPt, showed slight reversibility in their oxidation scans (Figure 4A) and were found to exhibit much lower IPs of 4.82−4.98 eV. (Table 2) This trend of reduced IPs in D−A conjugated polymers with stronger electron-accepting building blocks is consistent with previously reported theoretical calculations[3i] on various electron acceptors including BT, TP, PTP, and pyridine-based moieties. The calculated results showed that TP and PTP usually lowered the IP without a significant increase of the EA. This is in contrast to BT or other acceptors which tended to lower the IP while increasing the EA. Our experimental results confirm the theoretical prediction that TP-BTPt, PTP-BTPt, and MTP-BTPt should have similar EA values (3.03−3.21 eV) and smaller IP values (4.82−4.98 eV) compared to BT-BTPt.

The IPs of HPP-TP50 and HPP-TP67 are also affected by the presence of strong electron-accepting TP in their backbones, lowering their IPs to less than 5 eV. Furthermore, we can identify two oxidation peaks in HPP-TP50 and HPP-TP67 at 0.72−0.73 V and 0.94−0.98 V (vs SCE) as shown in Figure 4E, which originate from the thiophene units in the copolymers, respectively. In the case of HPP-PTP71 with an IP of 5.12 eV, the effect of PTP is not obvious due to the small amount of PTP in the copolymer. BT-MTP50 had an IP of 5.19 eV, which is close to that of BT-BTPt (5.15 eV). In the case of BT-F50 and BT-T50, their copolymer backbones were designed to introduce more electron-donating moieties such as thiophene−fluorene and bithiophene groups shown in Chart 2 to enhance

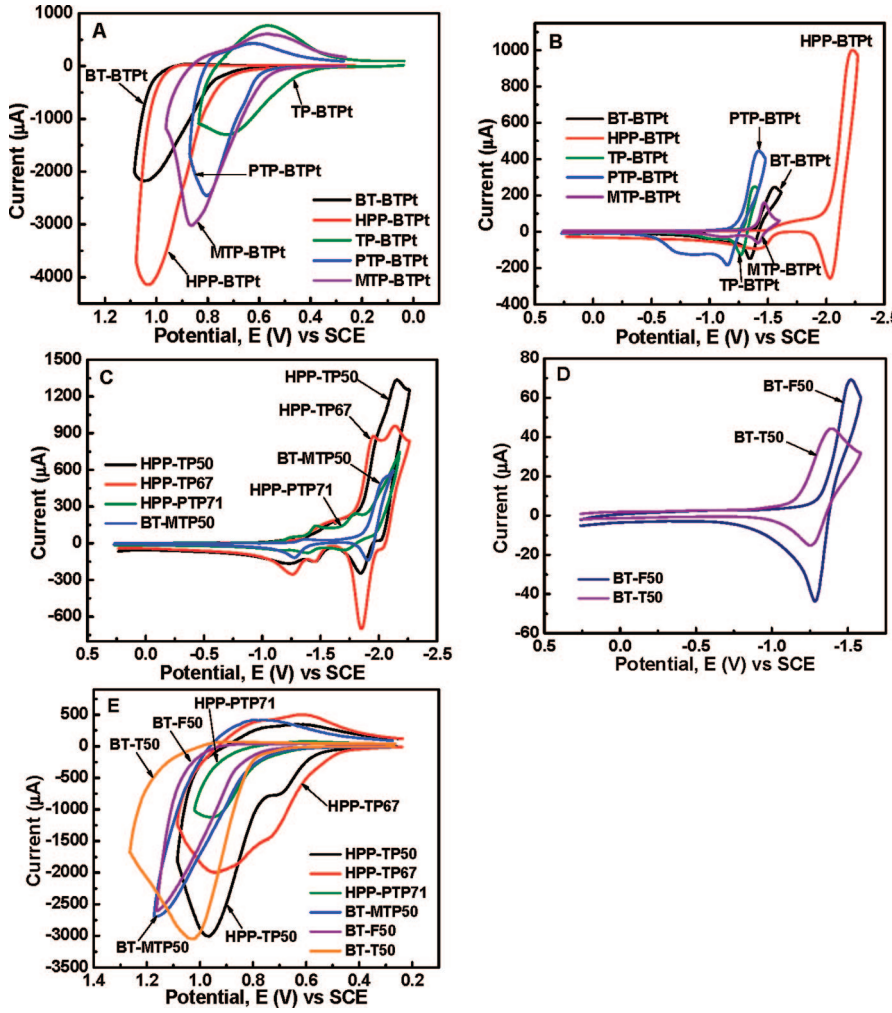

Figure 4. Cyclic voltammograms of thin films of organometallic copolymers in 0.1 M Bu_4NPF_6 solution in acetonitrile at a scan rate of 50 mV/s. Oxidation scans (A, E) and reduction scans (B, C, D).

their p-channel charge transport characteristics. Thus, BT-F50 and BT-T50 both exhibit quite high IPs of 5.23 and 5.20 eV as expected.

Based on our cyclic voltammograms of the series of organometallic copolymers, their electrochemical bandgaps can be calculated (E_g^{el} = IP − EA) and compared with the optical bandgaps (E_g^{opt}) listed in Table 2. The series of organometallic copolymers all share the same D−A−D architecture bridged by the electron-rich Pt ethynyl groups, among which the electron acceptor (A) is changed in order to modulate the ICT interactions between the D and A moieties. It is expected that the electrochemical bandgap will vary by the incorporation of different electron acceptors, similar to the optical bandgap. In general, the series of organometallic polymer semiconductors have small electrochemical bandgaps of 1.71−2.25 eV, which are 0.2−0.3 eV larger than the optical bandgaps (E_g^{opt} = 1.49−1.97 eV). This difference can be explained by the exciton binding energy of conjugated polymers which is typically in the range of ~0.4−1.0 eV.[14] Thus, the electrochemical bandgaps of the thieno[3,4-*b*]pyrazines-based polymers TP-BTPt (1.71 eV), PTP-BTPt (1.77 eV), and MTP-BTPt (1.93 eV) are much smaller than those of BT-BTPt (2.13 eV) and HPP-BTPt (2.25 eV). To be mentioned, HPP-TP50, HPP-TP67, and HPP-PTP71 exhibit lower E_g^{el} (1.80−1.85 eV) than that of HPP-BTPt (2.25 eV) because of the presence of TP or PTP moieties. BT-MTP50, BT-F50, and BT-T50 showed almost the same E_g^{el} (2.03−2.14 eV) with BT-BTPt (2.13 eV), attributed to the same Th-BT-Th pair in their molecular structures.

Field-Effect Charge Transport. The field-effect carrier mobilities of the organometallic conjugated D−A polymers were investigated by fabricating and evaluating thin film organic field-effect transistors (OFETs).[15,16] Among OFETs prepared from the eleven polymers, we observed p-channel characteristics in nine polymers but no charge transport was observed in devices made from PTP-BTPt and HPP-PTP71. The polymers showed typical p-channel output characteristics when operated in the accumulation mode.[15,16] In the saturated region, the source-drain current (I_D) and gate voltage (V_G) can be related to device and material parameters by the following equation:[15] $I_D = (W/2L)C_0\mu_h(V_G - V_T)^2$, where μ_h is the field-effect hole mobility, W is the channel width, L is the channel length, C_0 is the capacitance per unit area of the gate dielectric layer (SiO_2), and V_T is the threshold voltage. The saturation region field-effect mobility was calculated from the transfer characteristics of the OFETs by ploting $I_D^{1/2}$ vs V_G. The resulting average hole mobilities from measurements on 5−6 different devices are listed in Table 2. The average film thickness of the polymer in OFETs was measured to be 30−100 nm depending on the material and processing conditions.

The average field-effect hole mobility of BT-BTPt was found to be 1.83×10^{-5} cm^2/(V s), which is comparable with the reported time-of-flight hole mobility ($<2 \times 10^{-5}$ cm^2/(V s)) obtained from the BT-BTPt:PCBM (1:4) blend system.[7] The OFET output and transfer characteristics of these organometallic polymers are exemplified by the results in Figure 5 for a MTP-BTPt field-effect transistor processed from $CHCl_3$. Good drain-

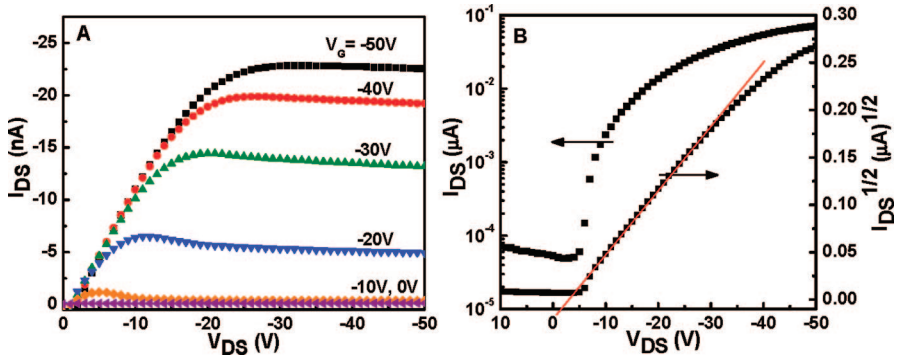

Figure 5. Output (A) and transfer (B) characteristics of an OFET fabricated from MTP-BTPt.

current modulation and well-defined linear and saturation regions are observed (Figure 5). A saturation region mobility of 8.47 $\times$ 10^{-5} $cm^2/(V\ s)$ with an on/off current ratio of 10^3 and a threshold voltage of -2.9 V were obtained for the MTP-BTPt OFET. The average hole mobilities of BT-BTPt and MTP-BTPt (μ_h = 1.83 $\times$ 10^{-5} and 3.32 $\times$ 10^{-5} $cm^2/(V\ s)$) are one to 2 orders of magnitude higher than those of the other polymers (3.87 $\times$ 10^{-7} to 6.27 $\times$ 10^{-6} $cm^2/(V\ s)$). The low mobilities of some of these polymers may be due to their low molecular weights since carrier mobility is a strong function of polymer molecular weight.[17] Another important factor that can explain the rather low carrier mobilities of these polymers is the large bulky side chains which likely impede close chain packing. The carrier mobility in even the highly crystalline regioregular poly(3-alkylthiophene)s is known to decrease strongly with increasing side chains beyond hexyl groups.[18]

The low IPs of the polymers (4.82−5.23 eV) facilitated hole injection and transport with respect to the gold source/drain electrodes (Φ = 5.1 eV) in the OFETs. However, although the CV scans clearly showed ambipolar redox properties, n-channel FET characteristics were not observed in any of the eleven organometallic polymer semiconductors. This is not surprising given the gold source/drain electrodes and that the measurements were done under ambient air; only a few examples of n-channel polymer OFETs are known to function in air.[19] We also note the much lower current flow in the reduction scans in the cyclic voltammetry while the oxidation scans showed much larger current flow. This relative magnitude of the CV currents indicates that these polymers are much better p-type semiconductors than of the n-type, contrary to what may be concluded from the reversibility of the oxidation and reduction CV waves.

Photovoltaic Properties. Bulk heterojunction (BHJ) solar cells using fullerene derivatives, $PC_{61}BM$ or $PC_{71}BM$, and the organometallic polymers were investigated. The current density−voltage characteristics of three photovoltaic devices (BT-BTPt:$PC_{61}BM$, BT-BTPt:$PC_{71}BM$, and HPP-BTPt:$PC_{71}BM$) are shown in Figure 6 and the photovoltaic parameters for all the polymers, including open circuit voltage (V_{oc}), short-circuit current density (J_{sc}), fill factor (FF), and power conversion efficiency (PCE) are summarized in Table 3. BT-BTPt devices reached 1.4% PCE when blended with $PC_{61}BM$ and 2.41% PCE when blended with $PC_{71}BM$. Although the performance of BT-BTPT:$PC_{61}BM$ devices has recently been reported to be 4.4−5% PCE in the literature,[7] Janssen and co-workers have contested that this system could only reach 2.2% PCE at best for a 70-nm active layer in the device.[10a] Our PCE results for BT-BTPt:methanofullerene solar cells are clearly more closely matched to the calculated 2.2% PCE[10a] than to the prior experimental data.[7]

All polymer blends were prepared at the blend ratio of 1:4 for polymer:$PC_{61}BM$ (or $PC_{71}BM$), and the spin-coated thin film thickness was determined to be in the range of 60−80 nm. The

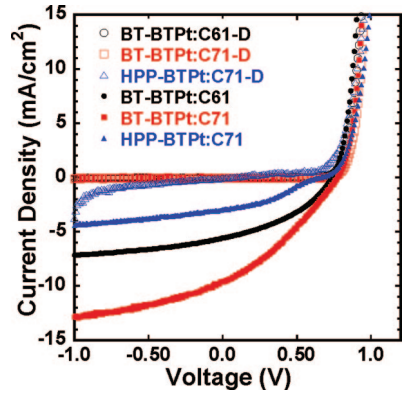

Figure 6. Current density−voltage ($J-V$) curves of solar cells using the polymer blends of BT-BTPt:$PC_{61}BM$ (or $PC_{71}BM$) and HPP-BTPt:$PC_{71}BM$ as active layers under simulated AM1.5 100 mW/cm^2 solar irradiation. $J-V$ curves under dark are also plotted for the same devices.

Table 3. Photovoltaic Parameters of Organometallic Polymers

polymer blend [a]	thickness (nm)	V_{oc} (V)	J_{sc} (mA/cm^2)	FF	PCE (%)
BT-BTPt:$PC_{71}BM$	75	0.77	9.65	0.32	2.41
HPP-BTPt:$PC_{71}BM$	80	0.66	2.99	0.34	0.68
TP-BTPt:$PC_{71}BM$	65	0.52	2.71	0.26	0.36
PTP-BTPt:$PC_{71}BM$	*b*	0.39	0.25	0.17	0.016
MTP-BTPt:$PC_{71}BM$	*b*	0.53	2.14	0.28	0.32
HPP-TP50:$PC_{61}BM$	60	0.50	1.39	0.23	0.16
HPP-TP67:$PC_{61}BM$	60	0.50	0.99	0.23	0.11
HPP-PTP71:$PC_{61}BM$	*b*	0.32	0.17	0.18	0.009
BT-MTP50:$PC_{71}BM$	*b*	0.52	0.86	0.25	0.11
BT-F50:$PC_{71}BM$	*b*	0.64	2.35	0.20	0.31
BT-T50:$PC_{71}BM$	*b*	0.68	4.21	0.25	0.71

[a] Polymer: $PC_{61}BM$ (or $PC_{71}BM$) = 1:4 for all blends. [b] The film thickness of these polymer:PCBM blends was in the range of 50−70 nm.

V_{oc} (0.77 V) for our BT-BTPt:$PC_{71}BM$ blend was close to 0.80−0.82 V previously reported for BT-BTPt devices.[7] The open-circuit voltage (V_{oc}) of the series of organometallic copolymers was found to be 0.66, 0.53, 0.52, and 0.39 V for HPP-BTPt: $PC_{71}BM$, MTP-BTPt: $PC_{71}BM$, PTP-BTPt:$PC_{71}BM$, and TP-BTPt:$PC_{71}BM$ devices (Table 3), respectively. The observed trend can be explained by the trend in the IP values of the organometallic polymers. Similarly, the V_{oc} values for the copolymer blends of HPP-TP50, HPP-TP67, and BT-MTP50 with fullerenes were also quite similar (0.50−0.52 V) since their IPs are comparable and limited by the incorporation of TP and MTP moieties. We note that the V_{oc} of PTP-BTPt and HPP-PTP71 blends were even lower (0.39 and 0.32 V), which may be due to their much lower IPs, molecular weights, and poor p-channel semiconducting behavior since no OFET characteristics were observed. In the copolymer blends utilizing

BT-F50 and BT-T50, their V_{oc} (0.64−0.68 V) were slightly lower than that of BT-BTPt (0.77 V). In general, some of the organometallic polymers showed quite low V_{oc}, which may be primarily due to their low IPs but also because of poor hole mobilities.

The short-circuit current density (J_{sc}) of the photovoltaic devices from the series of polymers is relatively low (0.17−4.21 mA/cm^2) except in BT-BTPt (9.65 mA/cm^2). However, our J_{sc} value is much lower than the reported 13.1−15.1 mA/cm^2 for BT-BTPt,[7] being the major limiting factor on our solar cell performance. The J_{sc} values calculated from the EQE measurements of BT-BTPt:$PC_{61}BM$ were 4.01 and 4.14 mA/cm^2 for two separate devices: the J_{sc} values calculated from the EQE measurements of BT-BTPt:$PC_{71}BM$ were 7.09 and 6.96 mA/cm^2 for two separate devices. They are in good agreement with the corresponding J_{sc} values calculated from the PCE measurement (Figure S11). We note that the J_{sc} is greatly reduced from BT-BTPt to HPP-BTPt, TP-BTPt, and MTP-BTPt for unclear reasons. Although the lower hole mobilities of HPP-BTPt and TP-BTPt are contributing factors, however, MTP-BTPt has a higher mobility than BT-BTPt and yet has a much lower J_{sc}. HPP-TP50 and HPP-TP67 have moderately high molecular weights but their hole mobilities were low, accounting for their rather poor J_{sc} values (1.39 and 0.99 mA/cm^2). Clearly, PTP-BTPt and HPP-PTP71 are poor p-type semiconductors for BHJ solar cells as a result of their low molecular weights and poor carrier mobilities. Even though additional electron-donating groups were incorporated into copolymers BT-F50 and BT-T50, their hole mobilities and J_{sc} were not improved.

The observed fill factor (FF) for BHJ solar cells incorporating these polymers as donors is generally low, in the 0.17−0.34 range. BT-BTPt and HPP-BTPt solar cells have comparable FF values of 0.32−0.34. The FF values for blends of fullerene with the other nine organometallic polymers were quite low (0.17−0.28), which may be a result of undesirable morphology in thin films. Although thienopyrazine-containing polymers (MTP-BTPt, TP-BTPt, PTP-BTPt) and copolymers (HPP-TP50, HPP-TP67, HPP-PTP71, BT-MTP50) have red-shifted and broader absorption spectra than BT-BTPt, which favor better photon energy absorption, their poor charge separation and charge transport clearly limit the power conversion efficiency.

The overall power conversion efficiency of the BHJ solar cells incorporating these organometallic polymers as donors and $PC_{71}BM$ (or $PC_{61}BM$) as acceptor varied widely among the polymers. The best efficiencies were 0.68−0.71% PCE observed for HPP-BTPt and BT-T50 and 2.41% PCE seen in BT-BTPt. Compared to regioregular poly(3-hexylthiophene)[9] and poly(3-butylthiophene)[20] donors for which hole mobilities exceeding 10^{-3} cm^2/(V s) have been observed in the context of BHJ devices, the orders of magnitude lower carrier mobilities in the present Pt-bridged organometallic polymers currently limit their photovoltaic properties.

Conclusions

Eleven Pt-bridged organometallic donor−acceptor conjugated polymers, incorporating various electron acceptors have been synthesized by a Sonogashira-type coupling polymerization and characterized. Most of the polymers had weight-average molecular weights (M_w) exceeding 10000, while some had M_w as large as 21000−58000, with polydispersity index around 2. By varying the electron-accepting strength in the donor−acceptor architecture, we demonstrate molecular engineering of the optical absorption bands, electronic band structure (HOMO/LUMO levels), charge transport, and photovoltaic properties. Although the absorption spectra of thienopyrazine-containing copolymers (MTP-BTPt, TP-BTPt, and PTP-BTPt) were broader than BT-BTPt due to the stronger effect of ICT, the improved light harvesting did not translate into improved photovoltaic properties. The observed ionization potentials of 4.82−5.23 eV facilitated the injection and transport of holes in the polymers, which showed field-effect hole mobilities of 3.87×10^{-7} to 3.32×10^{-5} cm^2/(V s). Electron transport was not observed and this is likely a result of the small electron affinities (2.95−3.28 eV). The highest photovoltaic power conversion efficiencies were observed in blends of the polymers with $PC_{71}BM$, ranging from 0.68−0.71% for HPP-BTPt and BT-T50 to 2.41% in BT-BTPt. Our observed 2.41% PCE for bulk heterojunction solar cells based on BT-BTPt as the donor is significantly lower than the previously reported 4.4−5.0% PCE[7] but is much closer to the theoretically estimated 2.2% PCE[10a] for this polymer.

Acknowledgment. This research was supported by the NSF (Grant DMR-0805259, DMR-0120967, DMR-0747489) and AFOSR EHSS MURI (Grant FA9550-06-1-0326).

Supporting Information Available: Figures showing ^{1}H NMR and MS spectral results, AFM images, and external quantum efficiency. This material is available free of charge via the Internet at http://pubs.acs.org.

References and Notes

(1) (a) Lee, B.-L.; Yamamoto, T. *Macromolecules* **1999**, *32*, 1375. (b) Yamamoto, T.; Zhou, Z. H.; Kanbara, T.; Shimura, M.; Kizu, K.; Maruyama, T.; Nakamura, Y.; Fukuda, T.; Lee, B.-L.; Ooba, N.; Tomaru, S.; Kurihara, T.; Kaino, T.; Kubota, K.; Sasaki, S. *J. Am. Chem. Soc.* **1996**, *118*, 10389. (c) Jenekhe, S. A.; Lu, L.; Alam, M. M. *Macromolecules* **2001**, *34*, 7315. (d) van Mullekom, H. A. M.; Vekemans, J. A. J. M.; Havinga, E. E.; Meijer, E. W. *Mater. Sci. Eng. R.* **2001**, *32*, 1. (e) Bunz, U. H. F. *Chem. Rev.* **2000**, *100*, 1605. (f) See the special issue on Organic Electronics: *Chem. Mater.* **2004**, *16*,4381−4846. (g) See the special issue on Organic Electronics and Optoelectronics: *Chem. Rev.* **2007**, *107*, 923−1386. (h) Kraft, A.; Grimsdale, A. C.; Holmes, A. B. *Angew. Chem., Int. Ed.* **1998**, *37*, 402.

(2) (a) Agrawal, A. K.; Jenekhe, S. A. *Macromolecules* **1993**, *26*, 895. (b) Agrawal, A. K.; Jenekhe, S. A. *Chem. Mater.* **1993**, *5*, 633. (c) Agrawal, A. K.; Jenekhe, S. A. *Chem. Mater.* **1996**, *8*, 579. (d) Cui, Y.; Zhang, X.; Jenekhe, S. A. *Macromolecules* **1999**, *32*, 3824. (e) Zhu, Y.; Yen, C.-T.; Jenekhe, S. A.; Chen, W.-C. *Macromol. Rapid Commun.* **2004**, *25*, 1829.

(3) (a) Yu, G.; Gao, J.; Hummelen, J. C.; Wudl, F.; Heeger, A. J. *Science* **1995**, *270*, 1789. (b) Jenekhe, S. A.; Yi, S. *Appl. Phys. Lett.* **2000**, *77*, 2635. (c) Alam, M. M.; Jenekhe, S. A. *J. Phys. Chem. B* **2001**, *105*, 2479. (d) Alam, M. M.; Jenekhe, S. A. *Chem. Mater.* **2004**, *16*, 4647. (e) Sonmez, G.; Shen, C. K. F.; Rubin, Y.; Wudl, F. *Adv. Mater.* **2005**, *17*, 897. (f) Campos, L. M.; Tontcheva, A.; Günes, S.; Sonmez, G.; Neugebauer, H.; Sariciftci, N. S.; Wudl, F. *Chem. Mater.* **2005**, *17*, 4031. (g) Svensson, M.; Zhang, F; Veenstra, S. C.; Verhees, W. J. H.; Hummelen, J. C.; Kroon, J. M.; Inganäs, O.; Andersson, M. R. *Adv. Mater.* **2003**, *15*, 988. (h) Admassie, S.; Inganäs, O.; Mammo, W.; Perzon, E.; Andersson, M. R. *Synth. Met.* **2006**, *156*, 614. (i) Blouin, N.; Michaud, A.; Gendron, D.; Wakim, S.; Blair, E.; Neagu-Plesu, R.; Belletête, M.; Durocher, G.; Tao, Y.; Leclerc, M. *J. Am. Chem. Soc.* **2008**, *130*, 732. (j) Thompson, B. C.; Fréchet, J. M. J. *Angew. Chem., Int. Ed.* **2008**, *47*, 58. (k) Günes, S.; Neugebauer, H.; Sariciftci, N. S. *Chem. Rev.* **2007**, *107*, 1324.

(4) (a) Zhang, X.; Jenekhe, S. A. *Macromolecules* **2000**, *33*, 2069. (b) Kulkarni, A. P.; Zhu, Y.; Jenekhe, S. A. *Macromolecules* **2005**, *38*, 1553. (c) Ego, C.; Marsitzky, D.; Becker, S.; Zhang, J.; Grimsdale, A. C.; Müllen, K.; MacKenzie, J. D.; Silva, C.; Friend, R. H. *J. Am. Chem. Soc.* **2003**, *125*, 437. (d) Wu, W.-C.; Liu, C.-L.; Chen, W.-C. *Polymer* **2006**, *47*, 527. (e) Thompson, B. C.; Madrigal, L. G.; Pinto, M. R.; Kang, T.-S.; Schanze, K. S.; Reynolds, J. R. *J. Polym. Sci., Part A: Polym. Chem.* **2005**, *43*, 1417. (f) Hancock, J. M.; Gifford, A. P.; Zhu, Y.; Lou, Y.; Jenekhe, S. A. *Chem. Mater.* **2006**, *18*, 4924.

(5) (a) Zhu, Y.; Champion, R. D.; Jenekhe, S. A. *Macromolecules.* **2006**, *39*, 8712. (b) Champion, R. D.; Cheng, K.-F.; Pai, C.-L.; Chen, W.-C.; Jenekhe, S. A. *Macromol. Rapid Commun.* **2005**, *26*, 1835. (c) Babel, A.; Wind, J. D.; Jenekhe, S. A. *Adv. Funct. Mater.* **2004**, *14*, 891. (d) Yamamoto, T.; Yasuda, T.; Sakai, Y.; Aramaki, S. *Macromol. Rapid Commun.* **2005**, *26*, 1214. (e) Yamamoto, T.; Kokubo, H.; Kobashi, M.; Sakai, Y. *Chem. Mater.* **2004**, *16*, 4616. (f) Chen, M.; Crispin, X.; Perzon, E.; Andersson, M. R.; Pullerits, T.; Andersson,

M.; Inganäs, O.; Berggren, M. *Appl. Phys. Lett.* **2005**, *87*, 252105. (g) Hancock, J. M.; Gifford, A. P.; Champion, R. D.; Jenekhe, S. A. *Macromolecules* **2008**, *41*, 3588. (h) Pang, H.; Skabara, P.; Crouch, D. J.; Duffy, W.; Heeney, M.; McCulloch, I.; Coles, S. J.; Horton, P. N.; Hursthouse, M. B. *Macromolecules* **2007**, *40*, 6585.

(6) Wong, W. Y. *J. Inorg. Organomet. Polym. Mater.* **2005**, *15*, 197.

(7) (a) Wong, W. Y.; Wang, X. Z.; He, Z.; Djurišić, A. B.; Yip, C. T.; Cheung, K. Y.; Wang, H.; Mak, C. S. K.; Chan, W. K. *Nat. Mater.* **2007**, *6*, 521. (b) The polymer BT-BTPt in Chart 1 was named **P1** in ref 7a.

(8) (a) Wong, W.-Y.; Wang, X.-Z.; He, Z.; Chan, K.-K.; Djurišić, A. B.; Cheung, K.-Y.; Yip, C.-T.; Ng, A. M.-C.; Xi, Y. Y.; Mak, C. S. K.; Chan, W.-K. *J. Am. Chem. Soc.* **2007**, *129*, 14372. (b) Wong, W.-Y. *Macromol. Chem. Phys.* **2008**, *209*, 14.

(9) (a) Kim, J. Y.; Kim, J. Y.; Kim, S. H.; Lee, H.-H.; Lee, K.; Ma, W.; Gong, X.; Heeger, A. J. *Adv. Mater.* **2006**, *18*, 572. (b) Reyes-Reyes, M.; Kim, K.; Carroll, D. J. *Appl. Phys. Lett.* **2005**, *87*, 083506. (c) Kim, Y.; Cook, S.; Tuladhar, S. M.; Choulis, S. A.; Nelson, J.; Durrant, J. R.; Bradley, D. D. C.; Giles, M.; McCulloch, I.; Ha, C.-S.; Ree, M. *Nat. Mater.* **2006**, *5*, 197.

(10) (a) Gilot, J.; Wienk, M. M.; Janssen, R. A. J. *Nat. Mater.* **2007**, *6*, 704. (b) Wong, W.-Y.; Wang, X.-Z.; He, Z.; Chan, K.-K.; Djurišić, A. B.; Cheung, K.-Y.; Yip, C.-T.; Ng, A. M.-C.; Xi, Y. Y.; Mak, C. S. K.; Chan, W.-K. *Nat. Mater.* **2007**, *6*, 704.

(11) Reddinger, J. L.; Reynolds, J. R. *Chem. Mater.* **1998**, *10*, 1236.

(12) Takahashi, S.; Kuroyama, Y.; Sonogashira, K.; Hagihara, N. *Synthesis* **1980**, 627.

(13) (a) Yang, C. J.; Jenekhe, S. A. *Macromolecules* **1995**, *28*, 1180. (b) Kulkarni, A. P.; Tonzola, C. J.; Babel, A.; Jenekhe, S. A. *Chem. Mater.* **2004**, *16*, 4556.

(14) Sariciftci, N. S. *Primary Photoexcitations in Conjugated Polymers: Molecular Excitons vs Semiconductor Band Model*; World Scientific: Singapore, 1997.

(15) Sze, S. M. *Physics of Semiconductor Devices*; Wiley: New York, 1981.

(16) (a) Ahmed, E.; Briseno, A. L.; Xia, Y.; Jenekhe, S. A. *J. Am. Chem. Soc.* **2008**, *130*, 1118. (b) Babel, A.; Jenekhe, S. A. *Macromolecules* **2003**, *36*, 7759.

(17) Kline, R. J.; McGehee, M. D.; Kadnikova, E. N.; Liu, J.; Frechet, J. M. J.; Toney, M. F. *Macromolecules* **2005**, *38*, 3312.

(18) Babel, A.; Jenekhe, S. A. *Synth. Met.* **2005**, *148*, 169.

(19) (a) Babel, A.; Jenekhe, S. A. *J. Am. Chem. Soc.* **2003**, *125*, 13656. (b) Briseno, A. L.; Mannesfeld, S. C. B.; Shamberger, P. J.; Ohuchi, F. S.; Bao, Z.; Jenekhe, S. A.; Xia, Y. *Chem. Mater.* **2008**, *20*, 4712.

(20) (a) Xin, H.; Kim, F. S.; Jenekhe, S. A. *J. Am. Chem. Soc.* **2008**, *130*, 5424. (b) Xin, H.; Kim, F. S.; Ren, G.; Jenekhe, S. A. *Chem. Mater.* **2008**, *20*, 6199.

MA8016508